Role of Tip Chemical Reactivity on Atom Manipulation Process in Dynamic Force Microscopy

Yoshiaki Sugimoto,[†,*] Ayhan Yurtsever,[†,‡] Masayuki Abe,[†,§] Seizo Morita,[†,‡] Martin Ondráček,[⊥] Pablo Pou,[∥] Ruben Pérez,[∥] and Pavel Jelínek[⊥]

[†]Graduate School of Engineering, Osaka University, 2-1 Yamada-Oka, Suita, Osaka 565-0871, Japan, [‡]Institute of Scientific and Industrial Research, Osaka University, 8-1 Mihogaoka, Ibaraki, Osaka 567-0047, Japan, [§]Graduate School of Engineering, Nagoya University, Furo-cho, Chikusa-ku, Nagoya 464-8603, Japan, [⊥]Institute of Physics, Academy of Sciences of the Czech Republic, Cukrovarnická 10/112, Prague, 162 00, Czech Republic, and [∥]Departamento de Física Teórica de la Materia Condensada and Condensed Matter Physics Center (IFIMAC), Universidad Autónoma de Madrid, E-28049 Madrid, Spain

ABSTRACT The effect of tip chemical reactivity on the lateral manipulation of intrinsic Si adatoms toward a vacancy site on a Si(111)-(7×7) surface has been investigated by noncontact atomic force microscopy at room temperature. Here we measure the atom-hopping probabilities associated with different manipulation processes as a function of the tip–surface distance by means of constant height scans with chemically different types of tips. The interactions between different tips and Si atoms are evaluated by force spectroscopic measurements. Our results demonstrate that the ability to manipulate Si adatoms depends extremely on the chemical nature of the tip apex and is correlated with the maximal attractive force measured over Si adatoms. We rationalize the observed dependence of the atom manipulation process on tip-apex chemical reactivity by means of density functional theory calculations. The results of these calculations suggest that the ability to reduce the energy barrier associated with the Si adatom movement depends profoundly on tip chemical reactivity and that the level of energy barrier reduction is higher with tips that exhibit high chemical reactivity with Si adatoms. The results of this study provide a better way to control the efficiency of the atomic manipulation process for chemisorption systems.

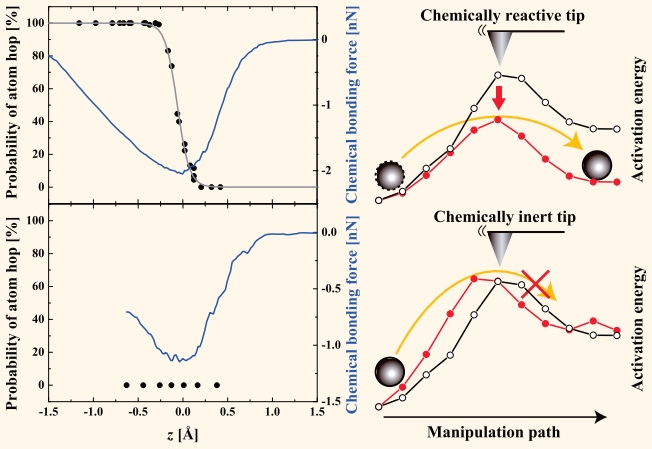

KEYWORDS: noncontact atomic force microscopy · dynamic force microscopy · atomic manipulation · force spectroscopy · chemical interaction force · density functional theory · nudged elastic band

Atomic force microscopy (AFM) has been developed into a versatile tool that can characterize various nanostructures and sample surfaces, including insulators. Atomic resolution can now be routinely obtained by using the frequency modulation technique, wherein a cantilever is oscillated at its resonance frequency (f_0), and the frequency shift (Δf) caused by the tip–surface interaction force is detected.[1,2] Other than the surface imaging capability, the interaction forces between the tip-apex atoms and individual surface atoms can be quantified by measuring the tip–surface distance dependence of the Δf [$\Delta f(z)$] curves,[3] in so-called force spectroscopy (FS). Single-atom chemical identification can thus be realized on the basis of FS measurements.[4,5]

In addition to these capabilities, AFM offers the fascinating ability to manipulate individual atoms[6−13] and molecules.[14−16] More importantly, AFM provides an opportunity to directly measure the driving forces involved in the atom manipulation process. A precise quantification of the forces required to manipulate the metal adsorbates on metal surfaces has been demonstrated by Ternes *et al.*[8] It was revealed that the manipulation process is determined mainly by the lateral force component, which is in contrast to the underlying mechanisms governing the manipulation process on semiconductor surfaces, where vertical force

* Address correspondence to sugimoto@afm.eei.eng.osaka-u.ac.jp.

Received for review June 19, 2013 and accepted July 26, 2013.

Published online August 01, 2013
10.1021/nn403097p

plays a dominant role.[7] This striking difference was attributed to the presence of highly directional covalent bonds on semiconductor surfaces.

The measurement of forces during the manipulation process provides the signatures of specific mechanical atom manipulation processes. These signatures have also been investigated to deduce the atomistic dynamics of these processes.[7,8,13,17] The triggering mechanism for atomic motion in the attractive tip−sample interaction regime has been attributed mainly to local energy barrier reduction induced by interaction forces between the tip and surface atoms.[7,17−19]

Despite these advances, further investigations are needed to elucidate the relationship between the mechanical atom manipulation capability and the role that the tip plays. It has been known that the manipulation processes are often influenced by details of the tip termination (*i.e.*, structures, orientations, and chemical natures).[17] The lack of successful atom manipulation and/or the varying success rates are attributable mainly to the tip properties. In order to increase the efficiency of the atomic manipulation process, a detailed understanding of the tips exhibiting different interaction characteristics is therefore required. In this context, there is only a recent work by Jarvis *et al.*,[20] which theoretically studies the role of the dangling bond orientation at the tip apex in the vertical atom manipulation process on a hydrogen-passivated Si(100) surface. It was shown that different tip types experience very different responses during the atom manipulation process due to differences in the alignment of their atomic orbitals with respect to that of the surface adatoms. In this paper, we tackle the problem of the influence of tip chemical reactivity on atom manipulation by combining room-temperature FS and AFM manipulation experiments with density functional theory (DFT) simulations on Si(111)-(7×7) surfaces.

We measure the probability of displacing a Si adatom to a vacancy site on the Si(111)-(7×7) surface as a function of the tip−sample distance. The statistics of the lateral manipulation of intrinsic Si adatoms for various processes are produced using a large variety of tips that span a broad range of attractive force maxima over the Si adatoms. We found that the atom manipulation capability and its efficiency in this particular manipulation process are strongly dependent on the maximal force of a tip acting on the Si adatom. DFT calculations reveal that the ability to reduce the local energy barrier required for adatom manipulation depends on the tip apex chemical reactivity.

RESULTS AND DISCUSSION

We studied the lateral manipulation of intrinsic Si adatoms on the Si(111)-(7×7) surface including an atomic vacancy as an open space. The AFM manipulation procedures and the experimental setup are detailed in the Methods section and in the Supporting Information. Briefly, the atom manipulation process was carried out by successive tip scans above the line along the [1$\bar{1}$0] direction (the left-right arrow) involving a vacancy as schematically illustrated in Figure 1A. To obtain reliable statistics on the atom manipulation procedure at well-defined distances, the tip is scanned at constant heights without tip−surface distance feedback while the Δf signal is recorded. To carry out a statistical analysis and to investigate the tip dependence of the observed manipulation process, we repeated the same experiment using 10 cantilevers with 15 different tip states, some of which were produced by gently contacting the tip to the sample surface. Such a comprehensive study comprising a large number of data sets acquired with different tips has not been reported previously for AFM manipulation experiments.

Figure 1 (C_1−H_2) shows the constant height Δf images of successive line scans above the same line on the Si(111)-(7×7) surface with the passage of time, which were obtained at different tip−sample distances using a certain type of tip. We should emphasize that the Δf images in each frame are obtained by repeatedly scanning the tip along the same line for both fast scan directions with the passage of time. The fast scan direction passes through from left to right (C_1−H_1) and right to left (C_2−H_2). While the Δf images in C_1 and C_2 are obtained at a large tip−sample distance, the Δf images in H_1 and H_2 are acquired at the closest tip−sample distance. The observed bright and continuous stripes as well as the intermittent stripes in the Δf images indicate the registry of the Si adatom position during the manipulation process. The success of the manipulation process could be inferred from the pattern of Δf images and from the line profiles.

When the tip was repeatedly scanned at sufficiently small tip−surface distances, the Si adatoms changed their adsorption locations among the corner adatom (Co), metastable (M), and center adatom (Ce) sites by interaction with the tip. Under the same experimental conditions (tip−sample distance and scan parameters), various types of line profiles corresponding to different atom-hopping processes are observed, which can be attributed to the stochastic nature of the hopping processes at room temperature.[10] In Figure 1B, we plot two exemplary manipulation profiles along the lines as highlighted in the Δf image in Figure 1E_1. From these line profiles, we witness two different outcomes starting from the same initial atom configuration. Under the same scan conditions, while the profile with triangles does not show any signature for adatom displacement and a vacancy stays on the Ce site, the profile with circles shows the signature for atom movement. During the tip passing over the left corner adatom, the Si adatom hops to the M site to follow the tip, leading to a jump in the Δf signal (at x = 17.8 Å). Then, the adatom hops from the M site to the Ce site successively (x = 20.7 Å). After this process, the vacancy is located on the left Co site.

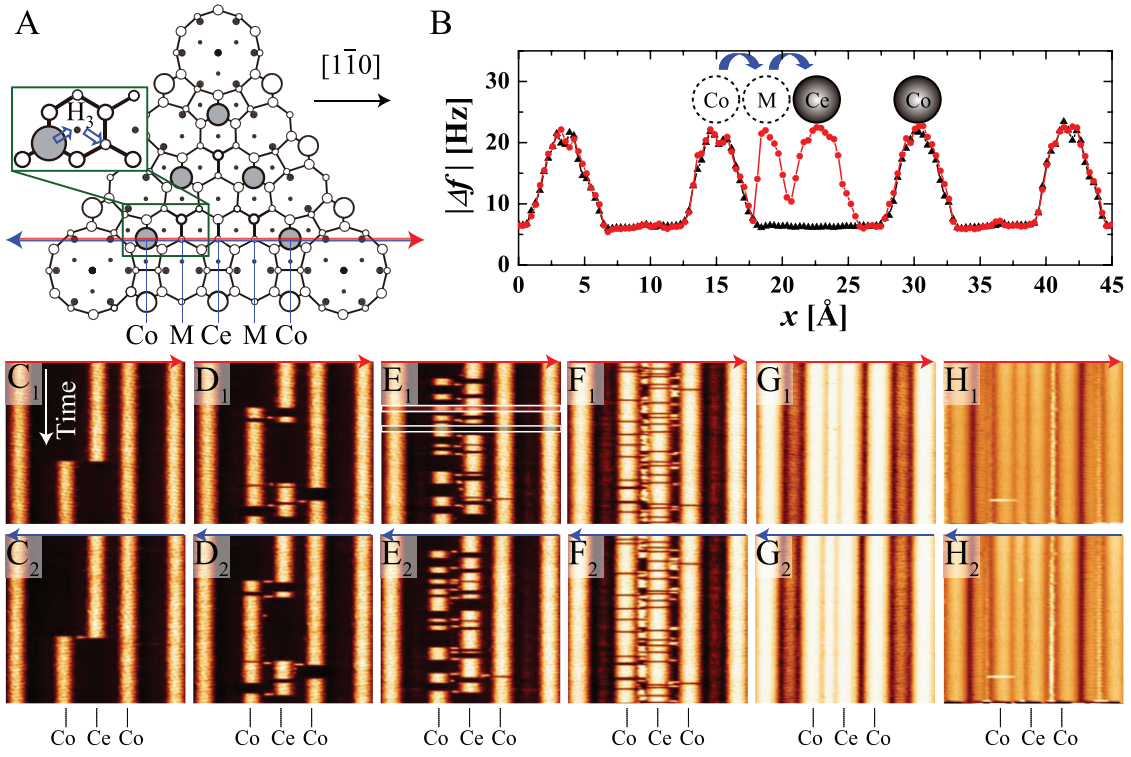

Figure 1. Manipulation of Si adatom at constant height by line scans. (A) Schematic model of a half unit cell in the Si(111)-(7×7) surface including a vacancy on a Ce site. The zoom out indicates the detail of the most favorable adatom hopping path (Co → H_3 → M). Successive tip scans above the line comprising a vacancy are carried out in both the forward and backward scan directions as indicated by the left-right arrow. (B) Two exemplary Δf line profiles extracted from the Δf image in panel E_1, revealing the dynamics of the Si adatom during the manipulation process acquired with the same scan parameters. The line profile indicated with black triangles does not show the atom hopping signature, while the profile with red circles shows atom hopping from a Co to a Ce site *via* the M site. (C_1−H_2) Constant height Δf images measured with the passage of time at different tip−sample distances for successive line scans along the fast scan direction passing from left to right (C_1−H_1) and right to left (C_2−H_2). Corresponding distances of the Δf images: (C_1, C_2) z = 0.21 Å, (D_1, D_2) z = 0.12 Å, (E_1, E_2) z = 0.02 Å, (F_1, F_2) z = −0.17 Å, (G_1, G_2) z = −0.31 Å, and (H_1, H_2) z = −1.16 Å. The z values were determined from the force curves shown in Figure 2A.

Relationship between the Measured Force Magnitude and Atom Manipulation Capability. In order to evaluate the atom-hopping probability associated with different manipulation processes, we analyzed line profiles extracted from the Δf images. We define the hopping probability as the ratio of the number of successful atom movements to the total number of line scans (*i.e.*, manipulation attempts), represented as a percentage. By analyzing more than 3000 line profiles in the Δf images acquired at various tip−surface distances using the tip used in Figure 1, we can obtain the tip−surface distance dependence of the hopping probability ascribed to the various processes. In Figure 2A, the probabilities of successful atom manipulation for three different processes are plotted as a function of the tip−surface distance. Each of these processes is illustrated schematically in the inset of Figure 2A. The short-range force curve [$F_z(z)$] and the potential energy curve [$U(z)$] are also indicated in Figure 2A and were calculated from the $\Delta f(z)$ curve measured above the Co adatom using the same tip (see Supporting Information). It should be emphasized that the force curves acquired over the Co adatom site can be used as a reference for the estimation of the tip−surface distances. The close proximity of the tip to the surface clearly affects atom manipulation. By bringing the tip into close proximity with the target atom, the atom-hopping probabilities increased drastically around the maximum attractive F_z region, from 0% to 100%.

We observed two different types of tips showing distinctly different abilities to manipulate Si adatoms. The tips in one group yielded atom manipulation around the maximum attractive F_z region, as mentioned above (see Figure 2A). On the other hand, the tips in the other group could not move atoms even when the tip approached the surface beyond the maximum attractive force region for any tip scan direction (see Figure 2B). Two types of tips can be switched by gentle tip−surface contacts even using the same cantilever. This was demonstrated in Figure 2C, which was obtained using the same cantilever after acquiring the data set in Figure 2B. After the modification of the tip-apex termination by controlled tip−surface contacts, the ability to move adatoms was successfully obtained. This implies that the property of the very end of the tip is an important parameter to determine the tip capability in atom movement.

We found that the ability to manipulate atoms depends significantly on the absolute values of the

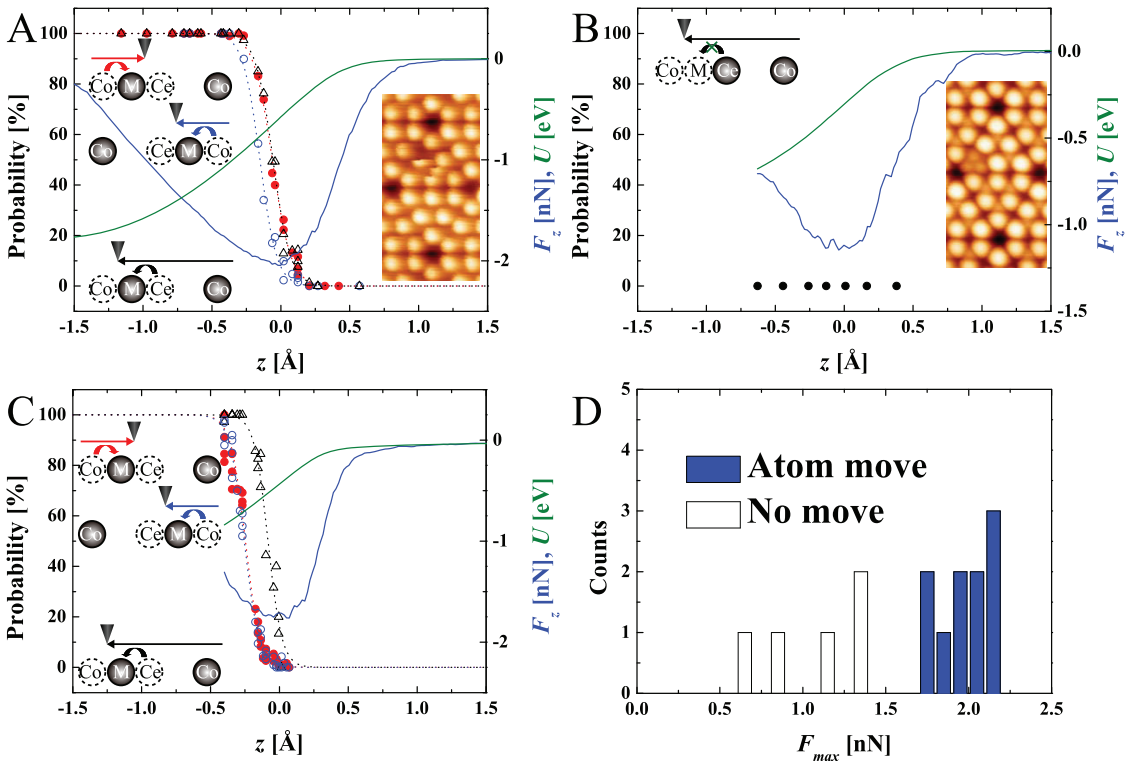

Figure 2. Atom manipulation probabilities associated with various processes obtained with different tips. (A) Tip−surface distance dependence of the atom hopping probability from the left Co to the M site (red solid circles), from the right Co to the M site (blue open circles), and Ce to the M site (black open triangles). The plots are fitted to an empirical step function, $P(z) = 100/[1 + \exp[\alpha(z - z_0)]]$, where α is the thermal broadening coefficient and z_0 is defined as the distance for $P = 50\%$. $F_z(z)$ and $U(z)$ curves obtained above the Co adatom using the same tip are also indicated. (B) Data set obtained using a different tip, which does not provide atom movement. The corresponding AFM topographic images produced by these two class of tips are shown in the insets in (A) and (B), respectively. (C) Data set obtained with the same cantilever as in (B), which is acquired after the tip state is modified by controlled tip−surface contacts, leading to a different tip state from that of the same cantilever. We note that the origin of the tip−surface distance ($z = 0$) is defined as the position of the minimum in the $F_z(z)$ curve. (D) Distribution of maximum attractive forces measured above Si adatoms, obtained using 15 different tips, revealing the relationship between the magnitude of F_{max} and the capability for atom manipulation.

maximum attractive F_z (F_{max}), which were measured above adatoms. We can categorize these two groups of tips in terms of their attractive force maxima over the Si adatoms. The statistical distribution of F_{max} provided by the interaction among 15 different tips with the Si adatom is displayed in Figure 2D, revealing the typical values of the forces and their distribution among the two groups of tips used in the manipulation experiments. Such a broad dispersion of F_{max} can be attributed to the varying degrees of tip-apex chemical reactivity, as previously reported in refs 21 and 22. The Si adatoms can be manipulated using the more reactive tips characterized by larger F_{max}, whereas manipulation is not observed using less reactive tips with smaller F_{max}. Two distinct characteristic behaviors of these tips in manipulating Si adatoms also manifest themselves in the AFM topographic images. The signatures attributed to the atom manipulation capabilities of the tips appear in the AFM topographic images where Si adatoms are easily displaced during scanning, as shown in the inset image in Figure 2A, and the Si rest atoms cannot be resolved in these images. On the other hand, the tips resolving the Si rest atoms together with adatoms have no ability to manipulate Si adatoms (see inset image in Figure 2B).

We also investigated the dependence of the manipulation probability on the scan directions in the equivalent manipulation process, *i.e.*, two symmetric manipulation pathways of Co to the M site (red and blue data points in Figure 2A). The investigation of the relative probabilities of equivalent manipulation processes is especially important in unraveling the details of the tip structures and in particular their symmetries. We found that the probability depends on the scan direction. The successful atom movement from left to right along the Co to the M site has a higher probability than that from the right to the left. These results can be attributed to the effect of tip asymmetry and/or the orientation of the tip-apex dangling bond with respect to the adatoms. A recent theoretical study suggested that the ability to vertically manipulate atoms on semiconductors depends strongly on the orientation of the dangling bonds at the tip apex with respect to the target atom.[20] Thus, the directional dependence of the dangling bond alignment (misalignment) with respect to the target atom leads to a variation in the

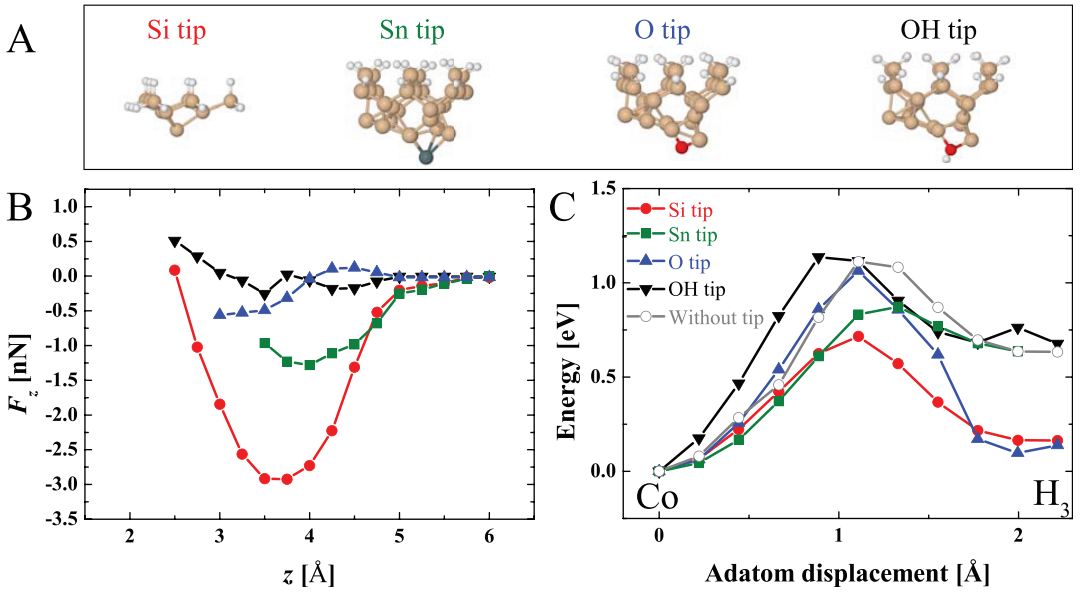

Figure 3. Role of tip chemical reactivity on the potential energy landscape for the displacement of an adatom adjacent to a vacancy on the Si(111)-(7×7) surface. (A) Ball-and-stick models of the tip apexes: Si tip, Sn-terminated tip, O-terminated tip, and OH-terminated tip. The color code for the ball-and-stick models is as follows: red corresponds to O, white to H, cream to Si, and dark blue to Sn. (B) F_z curves above the Co adatom obtained by DFT calculations using four different tip models that vary in chemical reactivity: Si tip (red), Sn-terminated tip (green), O-terminated tip (blue), and OH-terminated tip (black). (C) Variation in the potential energy profile for a Si adatom to hop from Co to the H_3 site when the tip was located at the midpoint between the Co and M sites, with vertical distance corresponding to the attractive force maxima of each force in (B). The energy barrier at the far tip−sample distance and/or in the absence of the tip is about 1.1 eV, calculated using a Si tip. Note that the extent of energy barrier reduction increases with the tip model exhibiting stronger attractive force maxima and higher chemical reactivity with the Si adatoms.

response to manipulation attempts, thus creating anisotropic behavior in the manipulation probability. Indeed, another experiment shown in Figure 2C—performed with a different tip—reveals that the rate of atom hopping along both of these directions is equally probable, thus pointing out the different tip symmetries.

DFT Calculations: Influence of Tip Chemical Reactivity on Energy Barrier Reduction. In order to complement the interpretation of the experimental observations, we carried out first-principles calculations to map out the interactions between several tips and the Si adatoms. The tip structures[23] represented by our models involve pure Si-based clusters grown in the (111) (Si-terminated tip) as well as in the (100) orientations (dimer) contaminated by the OH group (OH-terminated tip), Sn atom (Sn-terminated tip), and O atom (O-terminated tip), as depicted in Figure 3A. The results, summarized in Figure 3B, reveal a force magnitude of values ranging from 0.1 to 3 nN, which cover the ranges as encountered in the experimental force curves (see Figure 2D). These calculations show that the magnitude of the force is indicative of the degree of foremost apex atom reactivity with surface Si adatoms.[4,21] The tips made of pure Si clusters (Si tips) yield larger attractive forces on Si adatom sites, whereas the OH- and O-terminated tips, which are less reactive, create a smaller attraction to the Si adatoms. It is known that H adsorption on the Si adatom saturates the dangling bond states, which in turn can passivate the tip reactivity. On the other hand, the Sn-contaminated tip exhibits relatively higher chemical reactivity with Si adatoms with respect to passivated tips (*i.e.*, OH- and O-terminated tips).

In our previous DFT calculations,[7] we have shown that the attractive interaction with the tip induces vertical relaxation of Si adatoms to weaken the bonds with the backbond atoms, resulting in a reduction of the potential energy barrier for the adatom to thermally hop toward an adjacent empty adsorption site. This interpretation has been well recognized as the mechanism governing the manipulation process on semiconductor surfaces. To investigate the role that the tip chemical reactivity plays in this process, the energy barrier along the selected manipulation pathway connecting Co and the H_3 site, which a previous DFT calculation found to be the most favorable diffusion pathway,[7] was calculated by using the nudged elastic band (NEB) method[24] for the tip structures shown in Figure 3A.

The potential energy profiles calculated as a function of the adatom displacement along its favorable diffusion pathway are plotted in Figure 3C for various tip models with different chemical reactivities with surface Si adatoms. The calculation was performed under the influence of the tip located at the midpoint between Co and M sites (see Figure 1A) at a height corresponding to the attractive force maxima of the tips characterized in Figure 3B. The role of tip-apex chemical reactivity on the energy barrier reduction is clearly

evident in the surface energy landscape (see Figure 3C). The diffusion energy barrier at the far tip−sample distance regime (gray curve) is substantially reduced in the presence of a Si-terminated tip (red curve). On the other hand, the OH-terminated tip does not show any reduction in the potential energy barrier. In the same way, the O-terminated tip does not provide any remarkable reduction in the potential energy barrier. Indeed, the tip with a strong attractive force maximum, indicating higher tip reactivity, results in a larger reduction in the energy barrier.

We also investigated the generality of the basic trends observed in this study phenomenologically by extending the calculations to the Sn-terminated tip despite its absence in the measurement environment. The Sn-terminated tip exemplifies an intermediate case between a passivated OH tip and a reactive Si tip. This tip shows a maximum attractive force clearly larger than the passivated tips, but a smaller barrier reduction compared to the reactive Si tip. Moreover, adsorption of the Si adatom cannot be stabilized on the H_3 site in the case of the Sn-contaminated tip, due to the shallow minima at this site, which are deeper in the case of the more reactive Si tip. Considering the lower barrier reduction and the lack of stabilization of the H_3 minima, this tip can be classified into the group of tips that cannot displace atoms.

We found a strong correlation between the level of tip reactivity and the measure of the modification in the energy barrier reduction. With a chemically inert tip, the energy barrier cannot be reduced even at very close tip−adatom separations. In contrast, with a more chemically reactive tip, a significant reduction in the barrier height was observed. These results provide an explanation for the observed relationship between the atom manipulation ability and the magnitude of the attractive force maxima over the Si adatoms.

CONCLUSION

The role of AFM tips in vacancy-mediated lateral manipulation of Si adatoms on the Si(111)-(7×7) surface was systematically investigated using various different tips at room temperature. It was found that the ability to manipulate atoms is strongly correlated with the extent of tip reactivity, characterized by the magnitude of the maximum attractive force measured above a Si adatom. DFT calculations revealed that the lowering of the energy barrier required for adatom movement is strongly dependent on the extent of the chemical bonding force between the tip and the target atom. This suggests that the rate of atom manipulation on the semiconductor surface strongly depends on the extent of the tip-apex reactivity. We anticipate that the rate of successful manipulation of individual atomic species can be tuned by controlling the extent of tip chemical reactivity. Control of tip reactivity, therefore, can pave the way for efficient atom manipulation on semiconductor surfaces. We believe that this peculiarity is generally valid for the lateral manipulation of intrinsic adatoms that form covalent bonds with tips, *i.e.*, chemisorption-type systems.

METHODS

Experimental Details. The experiments were performed using a custom-built ultrahigh-vacuum AFM operated at room temperature. The AFM was operated using the frequency modulation detection mode,[25] keeping the cantilever oscillation amplitude constant. Commercial Si cantilevers prior to imaging and manipulation were cleaned by Ar ion sputtering in an ultra-high vacuum to remove native oxide layers and other contaminants. The cantilever oscillation amplitude (A) was set to be sufficiently large to operate the AFM stably. A sample voltage (V_s) with respect to the tip was applied such that electrostatic force was minimized.

Short-Range Force Measurements and Atom Manipulation Procedures. In the first stage, prior to the manipulation experiments, force spectroscopic measurements were carried out above a Si adatom to characterize the tip chemical reactivity. Force spectroscopy was carried out by recording the Δf with respect to the resonant frequency (f_0) as a function of the tip−sample distance (z). These measurements were acquired above an adatom with a lateral precision of 0.1 Å using the atom tracking method described elsewhere.[26] $\Delta f(z)$ curves were then converted to force−distance curves using the method described in ref 27. After compensating for the thermal drift using feedforward control,[28] the atom tracking system was then turned off, and successive line scans along the manipulation path comprising a vacancy and an Si adatom in the [1$\bar{1}$0] direction were performed. It is noteworthy to emphasize that precise adjustment of the scan line above the center of a vacancy and target adatom is required for successful atom manipulation. This was achieved using a versatile scan controller.[29] Detailed information on the experimental protocols and manipulation procedure used is given in the Supporting Information.

Computational Details. All total energy calculations were performed with the local orbital DFT code FIREBALL.[30] The calculations were performed within the local-density approximation (LDA) for the exchange−correlation functional. The valence electrons have been described by optimized[31] numerical atomic-like orbitals having the following cutoff radii (in au): Rc(s, s*) = 3.8 for H; Rc(s, s*) = 3.3, Rc(p, p*) = 3.8 for O; Rc(s) = 4.8, Rc(p) = 5.4, and Rc(d) = 5.2 for Si orbitals; Rc(s) = 5.2, Rc(p) = 5.7, and Rc(d) = 5.6 for Sn orbitals, respectively. The clean Si(111) surface was modeled in a 7×7 supercell geometry consisting of 347 atoms, with an atomic slab of six Si layers, and the back-side of the slab was passivated by H atoms. The Si equilibrium bulk lattice constant of 5.46 Å was used to build the slab geometry. The five top Si layers of the slab were allowed to relax, whereas the rest of the atoms were kept fixed during the optimization process. Individual geometries have been converged until the respective criteria of 10^{-6} eV and 0.05 eV/Å for the accuracy in energy and force were satisfied. The structural optimization calculations were carried out using only the G k-point sampling of the Brillouin zone.

Force *versus* distance calculations were performed using a quasi-static approach with different silicon-based tips.[23] The tip was gradually moved toward the surface in steps of 0.25 Å along the surface normal. At every such step all atoms of the Si(111)-7×7 surface and the AFM tip (except for the bottom layer of the slab and the base part of the tip) were allowed to relax to their ground-state configuration, fulfilling the convergence criteria specified above. The total short-range tip−sample forces were then determined as a sum of the final forces acting on the fixed atoms of the tip. The energy barriers for Si adatom movements were calculated using the nudged elastic band method.[24]

Conflict of Interest: The authors declare no competing financial interest.

Acknowledgment. This work was supported by a Grant-in-Aid for Scientific Research (22221006, 24360016, 24651116, 22760028, and 25106002) from the Ministry of Education, Culture, Sports, Science and Technology of Japan (MEXT), Funding Program for Next Generation World-Leading Researchers. P.J. and M.O. acknowledge the financial support of GAAV M100101207. M.O. acknowledges the support provided by the Czech Science Foundation (GACR) under the project P204/11/P578. R.P. and P.P. acknowledge MAT2011-23627, CSD2010-00024, CAM S2009/MAT-1467, and PLE2009-0061 (MINECO, Spain). P.P. was supported by the Ramon y Cajal program (MINECO, Spain).

Supporting Information Available: Additional information related to the experimental protocols; additional data sets for the probability of various manipulation processes, obtained using different tips. This material is available free of charge *via* the Internet at http://pubs.acs.org.

REFERENCES AND NOTES

1. Morita, S., Wiesendanger, R., Meyer, E., Eds. *Noncontact Atomic Force Microscopy*; Springer-Verlag: Berlin, 2002.
2. Giessibl, F. J. Advances in Atomic Force Microscopy. *Rev. Mod. Phys.* **2003**, *75*, 949–983.
3. Lantz, M. A.; Hug, H. J.; Hoffmann, R.; van Schendel, P. J. A.; Kappenberger, P.; Martin, S.; Baratoff, A.; Guntherodt, H. J. Quantitative Measurement of Short-Range Chemical Bonding Forces. *Science* **2001**, *291*, 2580–2583.
4. Sugimoto, Y.; Pou, P.; Abe, M.; Jelinek, P.; Perez, R.; Morita, S.; Custance, O. Chemical Identification of Individual Surface Atoms by Atomic Force Microscopy. *Nature (London)* **2007**, *446*, 64–67.
5. Setvin, M.; Mutombo, P.; Ondracek, M.; Majzik, Z.; Svec, M.; Chab, V.; Ostadal, I.; Sobotik, P.; Jelinek, P. Chemical Identification of Single Atoms in Heterogeneous III−IV Chains on Si(100) Surface by Means of nc-AFM and DFT Calculations. *ACS Nano* **2012**, *6*, 6969–6976.
6. Hirth, S.; Ostendorf, F.; Reichling, M. Lateral Manipulation of Atomic Size Defects on the CaF_2(111) Surface. *Nanotechnology* **2006**, *17*, S148–S154.
7. Sugimoto, Y.; Jelinek, P.; Pou, P.; Abe, M.; Morita, S.; Perez, R.; Custance, O. Mechanism for Room-Temperature Single-Atom Lateral Manipulations on Semiconductors Using Dynamic Force Microscopy. *Phys. Rev. Lett.* **2007**, *98*, 106104.
8. Ternes, M.; Lutz, C. P.; Hirjibehedin, C. F.; Giessibl, F. J.; Heinrich, A. J. The Force Needed to Move an Atom on a Surface. *Science* **2008**, *319*, 1066–1069.
9. Sugimoto, Y.; Pou, P.; Custance, O.; Jelinek, P.; Abe, M.; Perez, R.; Morita, S. Complex Patterning by Vertical Interchange Atom Manipulation Using Atomic Force Microscopy. *Science* **2008**, *322*, 413–417.
10. Sugimoto, Y.; Miki, K.; Abe, M.; Morita, S. Statistics of Lateral Atom Manipulation by Atomic Force Microscopy at Room Temperature. *Phys. Rev. B* **2008**, *78*, 205305.
11. Custance, O.; Perez, R.; Morita, S. Atomic Force Microscopy as a Tool for Atom Manipulation. *Nat. Nanotechnol.* **2009**, *4*, 803–810.
12. Yurtsever, A.; Sugimoto, Y.; Abe, M.; Matsunaga, K.; Tanaka, I.; Morita, S. Alkali-Metal Adsorption and Manipulation on a Hydroxylated TiO_2(110) Surface Using Atomic Force Microscopy. *Phys. Rev. B* **2011**, *84*, 085413.
13. Sweetman, A.; Jarvis, S.; Danza, R.; Bamidele, J.; Gangopadhyay, S.; Shaw, G. A.; Kantorovich, L.; Moriarty, P. Toggling Bistable Atoms *via* Mechanical Switching of Bond Angle. *Phys. Rev. Lett.* **2011**, *106*, 136101.
14. Mao, H. Q.; Li, N.; Chen, X.; Xue, Q. K. Mechanical Properties of H_2Pc Self-Assembled Monolayers at the Single Molecule Level by Noncontact Atomic Force Microscopy. *J. Phys.: Condens. Matter* **2012**, *24*, 084004.
15. Pawlak, R.; Fremy, S.; Kawai, S.; Glatzel, T.; Fang, H.; Fendt, L. A.; Diederich, F.; Meyer, E. Directed Rotations of Single Porphyrin Molecules Controlled by Localized Force Spectroscopy. *ACS Nano* **2012**, *6*, 6318–6324.
16. Langewisch, G.; Falter, J.; Fuchs, H.; Schirmeisen, A. Forces during the Controlled Displacement of Organic Molecules. *Phys. Rev. Lett.* **2013**, *110*, 036101.
17. Pizzagalli, L.; Baratoff, A. Theory of Single Atom Manipulation with a Scanning Probe Tip: Force Signatures, Constant-Height, and Constant-Force Scans. *Phys. Rev. B* **2003**, *68*, 115427.
18. Kurpick, U.; Rahman, T. S. Tip Induced Motion of Adatoms on Metal Surfaces. *Phys. Rev. Lett.* **1999**, *83*, 2765.
19. Kuhnle, A.; Meyer, G.; Hla, S. W.; Rieder, K. H. Understanding Atom Movement during Lateral Manipulation with the STM Tip Using a Simple Simulation Method. *Surf. Sci.* **2002**, *499*, 15–23.
20. Jarvis, S.; Sweetman, A.; Bamidele, J.; Kantorovich, L.; Moriarty, P. Role of Orbital Overlap in Atomic Manipulation. *Phys. Rev. B* **2012**, *85*, 235305.
21. Yurtsever, A.; Sugimoto, Y.; Tanaka, H.; Abe, M.; Morita, S.; Ondracek, M.; Pou, P.; Perez, R.; Jelinek, P. Force Mapping on a Partially H-Covered Si(111)-(7×7) Surface: Influence of Tip and Surface Reactivity. *Phys. Rev. B* **2013**, *87*, 155403.
22. Sharp, P.; Jarvis, S.; Woolley, R.; Sweetman, A.; Kantorovich, L.; Pakes, C.; Moriarty, P. Identifying Passivated Dynamic Force Microscopy Tips on H:Si(100). *Appl. Phys. Lett.* **2012**, *100*, 233120.
23. Pou, P.; Ghasemi, S. A.; Jelinek, P.; Lenosky, T.; Goedecker, S.; Perez, R. Structure and Stability of Semiconductor Tip Apexes for Atomic Force Microscopy. *Nanotechnology* **2009**, *20*, 264015.
24. Henkelman, G.; Jonsson, H. Improved Tangent Estimate in the Nudged Elastic Band Method for Finding Minimum Energy Paths and Saddle Points. *J. Chem. Phys.* **2000**, *113*, 9978–9985.
25. Albrecht, T. R.; Grütter, P.; Horne, D.; Rugar, D. Frequency Modulation Detection Using High-Q Cantilevers for Enhanced Force Microscope Sensitivity. *J. Appl. Phys.* **1991**, *69*, 668–673.
26. Abe, M.; Sugimoto, Y.; Custance, O.; Morita, S. Room-Temperature Reproducible Spatial Force Spectroscopy Using Atom-Tracking Technique. *Appl. Phys. Lett.* **2005**, *87*, 173503.
27. Sader, J. E.; Jarvis, S. P. Accurate Formulas for Interaction Force and Energy in Frequency Modulation Force Spectroscopy. *Appl. Phys. Lett.* **2004**, *84*, 1801.
28. Abe, M.; Sugimoto, Y.; Namikawa, T.; Morita, K.; Oyabu, N.; Morita, S. Drift-Compensated Data Acquisition Performed at Room Temperature with Frequency Modulation Atomic Force Microscopy. *Appl. Phys. Lett.* **2007**, *90*, 203103.
29. Horcas, I.; Fernandez, R.; Gomez-Rodriguez, J.; Colchero, J.; Gomez-Herrero, J.; Baro, A. WSXM: A Software for Scanning Probe Microscopy and a Tool for Nanotechnology. *Rev. Sci. Instrum.* **2007**, *78*, 013705.
30. Lewis, J. P.; Jelinek, P.; Ortega, J.; Demkov, A. A.; Trabada, D. G.; Haycock, B.; Wang, H.; Adams, G.; Tomfohr, J. K.; Abad, E.; *et al.* Advances and Applications in the FIREBALL ab Initio Tight-Binding Molecular-Dynamics Formalism. *Phys. Status Solidi B* **2011**, *248*, 1989–2007.
31. Basanta, M. A.; Dappe, Y. J.; Jelinek, P.; Ortega, J. Optimized Atomic-Like Orbitals for First-Principles Tight-Binding Molecular Dynamics. *Comput. Mater. Sci.* **2007**, *39*, 759–766.